ARCHIVES OF ACOUSTICS
11, 3, 287-298 (1986)

ULTRASONIC ECHO METHOD IN DETECTION OF BREAST CALCIFICATIONS. TRANSIENT ANALYSIS

LESZEK FILIPCZYŃSKI, TAMARA KUJAWSKA, GRAŻYNA ŁYPACEWICZ

Department of Ultrasonics, Institute of Fundamental Technological Research, Polish Academy of Sciences
(00-049 Warsaw, ul. Świętokrzyska 21)

The detectability of calcifications in women breast by means of the ultrasonic echo method was estimated on the basis of the transient analysis of the ultrasonic pulse reflection. Two calcification models in the form of a rigid and an elastic sphere were considered.

Echoes obtained at tissue inhomogeneities form an interference background which masks echoes from small calcifications. The level of the tissue interference background was determined on the basis of measurements in 100 femal breasts and it was shown that the obtained experimental results are probable from the theoretical point of view.

As the result of the performed analysis and experiments the author concluded that microcalcifications are not detectable by the ultrasonic echo method. The radii of calcifications which can be found at the frequency of 5 MHz are equal to 0.6 mm or 1.6 mm depending on the maximum sampling error assumed for a single measurement of the tissue interference background.

1. Introduction

The detection of microcalcifications is of basic significance in the early diagnosis of breast tumors. The reactions occurring in breast tissue cells causing calcifications in the case of tumors appear already at the very early stage of their development. In view of this the question of possibilites of detecting small calcifications by the ultrasonic method becomes one of essential significance. Two versions of this method, the echo and the shadow techniques are of interest [2].

In both cases examinations involve short ultrasonic pulses at frequencies usually contained between 3 and 5 MHz.

In previous papers [1], [2] the problem of calcification detection by means of the echo method was investigated on the basis of the steady-state analysis. The purpose of this paper is to extend the analysis of transient phenomena and to discuss in detail the obtained experimental results.

2. Assumptions

It is assumed for simplification that the calcifications are rigid or elastic sphereswith the radius a. The longitudinal wave velocity in the calcification and its density are assumed similarly to those for bone tissue, to be, respectively, $c_L = 3.2.$ km/s and $\varrho = 2.23$ g/cm^3 [14]. The literature contains no information on the velocity of transverse waves in bone tissue, therefore the value of Poisson ratio $v = 0.2$ will be assumed. In follows from Table 1 that this assumption

Table 1. Poisson's ratio v for various materials and the value assumed for the calcification

Material	v	Material	v
Lead	0.44	Bismuth	0.33
Gold	0.42	Nickel	0.31
Platinum	0.39	Cadmium	0.30
Silver	0.38	Steel	0.28
Brass	0.35	Glass (crown)	0.27
Perspex	0.35	Zinc	0.25
Tungsten	0.35	Glass (flint)	0.24
Copper	0.35	Porcelain	0.23
Constantan	0.33	Calcification	0.2
Ice	0.33	Fused quartz	0.17
Tin	0.33	Berylium	0.05

is most probably, when this value is compared with those of other materials. The wave velocity and the attenuation coefficient of the breast tissue is assumed to be $c_L = 1.5$ km/s and $a = 1.1$ dB/cm MHz, respectively. It is also assumed that pulse of a plane ultrasonic wave, composed of two high frequency 5 MHz periods, is incident on the spherical calcification.

To analyse the detection ability of the echo method with a typical ultrasonograph we assume its sensitivity to be 10 μV, the transmitter pulse voltage: 250 V and overall transducing losses (double piezoelectric transducing) equal to $T = -15$ dB.

3. The reflection of ultrasonic pulses from rigid and elastic spheres

The transient analysis of the ultrasonic pulse reflection enables us to find the smallest calcification size which is potentially detectable with a typical ultrasonograph (scanner). In our computations we applied the procedure as

presented by RUDGERS [11] and HICKLING [7] for pulse reflections from rigid and elastic spheres, respectively.

The acoustic pressure p_i of a plane continuous wave, travelling in the x direction, incident on the sphere, has the form

$$p_i = p_{i0} \exp[j(\omega t - kx)] \quad \text{or} \quad p_i = p_{i0} \exp[jk(ct - x)] \tag{1a, b}$$

where p_{i0} denotes the pressure amplitude, $\omega = 2\pi f$, f — frequency, t — time, $k = \omega/c$, c — wave velocity in the soft tissue.

The acoustic pressure p_s of the wave reflected from the sphere can be expressed as

$$p_s = p_{i0} \sum_{m=0}^{\infty} (2m+1)(-j)^m c_m h_m^{(2)}(kr) P_m(\cos\theta) \exp(j\omega t) \tag{2}$$

where m denotes natural number, $j = \sqrt{-1}$, $h_m^{(2)}(kr)$ — spherical Hankel function of second kind $P_m(\cos\theta)$ — Legendre polynominal, c_m — scatternig coefficient of the m-th partial wave, θ — azimuth. For the backward reflection $\theta = 180°$, $P_m(\cos\theta) = (-1)^m$. The function $h_m^{(2)}(kr)$ can be represented by the assymptotic expression (for $kr \gg 1$)

$$h_m^{(2)}(kr) = \frac{1}{kr} \exp\left[-j\left(kr - \frac{m+1}{2}\pi\right)\right]. \tag{3}$$

Thus, Eq. (2) becomes

$$p_{s0} = p_{i0} \frac{a}{2r} f_\infty(ka) \tag{4}$$

where

$$f_\infty(ka) = \frac{2j}{ka} \sum_{m=0}^{\infty} (2m+1)(-1)^m c_m(ka) \tag{5}$$

when $r \gg a$ [1], [7], [12]. p_{s0} denotes the pressure amplitude of the reflected wave.

Figs. 1 and 2 show the far field form function (for backward reflection) [7] $f_\infty(ka)$ which was computed Eq. (5). For computations of c_m formulae of HASEGAWA [6] were applied. The diagrams of the far field form function presented in Figs. 5 and 1 in the papers [1] and [2], respectively, are incorrect due to an error in the computing program.

In the case of a rigid sphere, the longitudinal and transverse wave velocities in the sphere tend to infinity. It can then be shown that Eq. (5) takes a much simpler form as $c_m = -j_m'(ka)/h_m^{(2)'}(ka)$, where $j_m'(ka)$ and $h_m^{(2)'}(ka)$ denote derivatives of spherical Bassel and Hankel functions with respect to the argument.

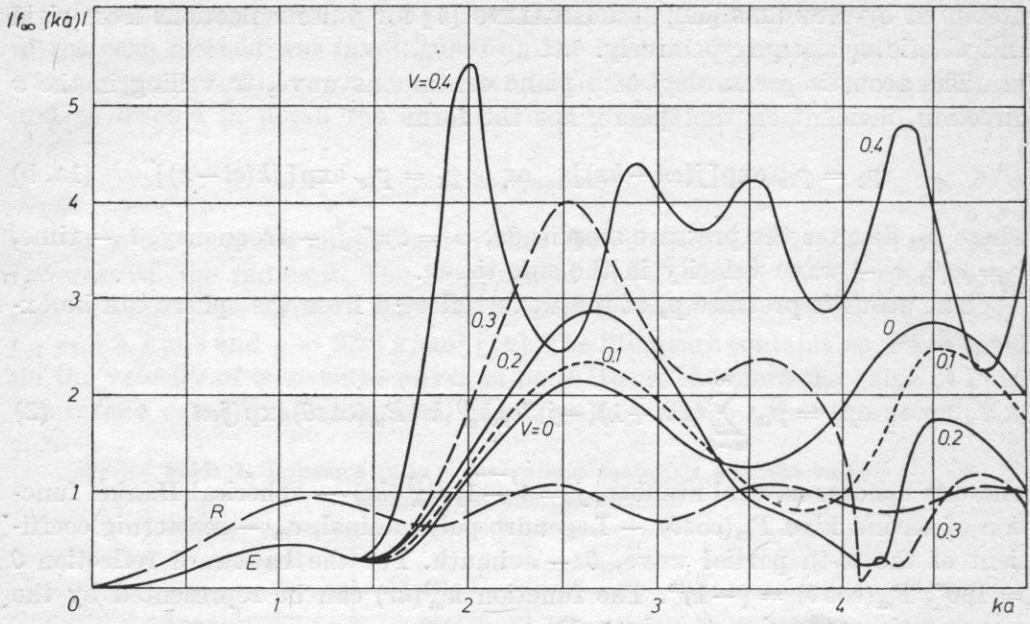

Fig. 1. Modulus of the far field form function $f_\infty(ka)$ (backward reflection) calculated for rigid (R) and elastic (E) spheres under consideration, v — Poisson's ratio

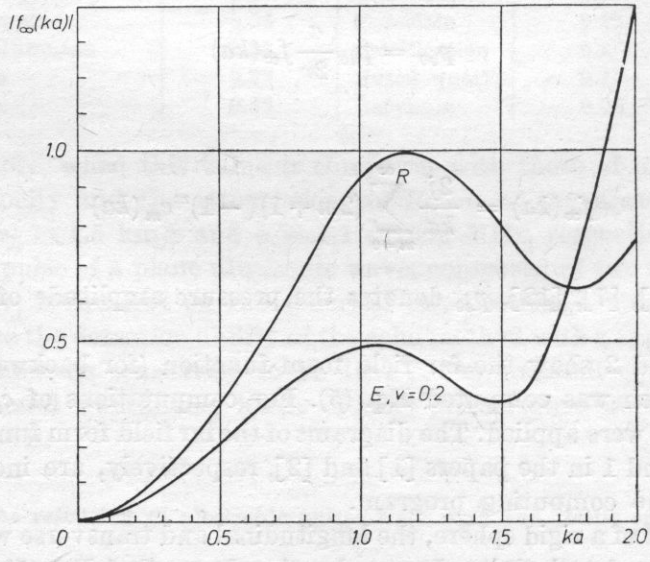

Fig. 2. Modulus of the function $f_\infty(ka)$ as in Fig. 1 but calculated for small arguments of ka ($v = 0{,}2$)

It follows from Eqs. (1a, b) that the acoustic pressure varies as a function of two variables, t and r. It is convenient to introduce one dimensionless variable in the form

$$\tau = (ct - r)/a \tag{6}$$

then Eq. (1b) becomes

$$p_i = p_{i0} \exp(jka\tau). \tag{7}$$

The last expression is valid for steady-state. In the case of transients the incident wave pulse can be represented in the form [11]

$$p_i = p_{i0} \prod (\tau/l - 1/2) \sin k_0 a\tau \tag{8}$$

where

$$\prod = \begin{cases} 1 \text{ when } |x| \leqslant 1/2, \\ 0 \text{ when } |x| > 1/2 \end{cases}$$

and $l = 2\pi b/k_0 a$ is the dimensionless pulse duration, b — number of high frequency periods, equals 2 in our case, k_0 — wave number corresponding to the carrier frequency of the incident wave pulse.

The incident wave pulse can be represented in the frequency domain as a function of a. However, in view of the form of Eqs. (7), (8), it will be given in a more general form, as a function of the dimensionless variable $\omega a/c = ka$. By using the inverse Fourier transform [8] the pulse reflected from the sphere can be represented in the form

$$p_s(\tau) = \frac{p_{i0}}{2\pi} \int_{-\infty}^{+\infty} \frac{a}{2r} f_\infty(ka) G_i(ka) \exp(jka\tau)\, d(ka) \tag{9}$$

where $G_i(ka)$ represents the spectrum of the incident pulse in the domain of ka, expressed as the Fourier transform of $p_i(\tau)$

$$G_i(ka) = \int_{-\infty}^{+\infty} p_i(\tau) \exp(-jka\tau)\, d\tau. \tag{10}$$

In Eq. (9), each monochromatic component of the incident pulse spectrum $G_i(ka)$ is weighted by the function $(a/2r)\, f_\infty(ka)$ [12] which represents the reflection spectral characteristics of the sphere.

Fig. 3 shows the reflected pulse shape computed as the real component from Eqs. (9), (10), (5), (8) for $k_0 a = 2.5$ ($f = 5$ MHz, $a = 0.12$ mm). Its relative amplitude is equal to 2.2, while the one of the reflected continuous wave, obtained directly from Fig. 1. equals 2.7. For $k_0 a = 1$ transient and steady-state analysis do not show any difference in the relative amplitude of the reflected wave being equal to 0.45.

The reflected pulse (Fig. 3) starts at $\tau = -2$, as this point corresponds to the pulse reflection from the anterior sphere surface ($r = a$) which takes place in the time $t = -a/c$. For our time coordinate starts at the instant in which the incident wave arrives at the sphere center, i.e., $t = 0$ for $r = 0$.

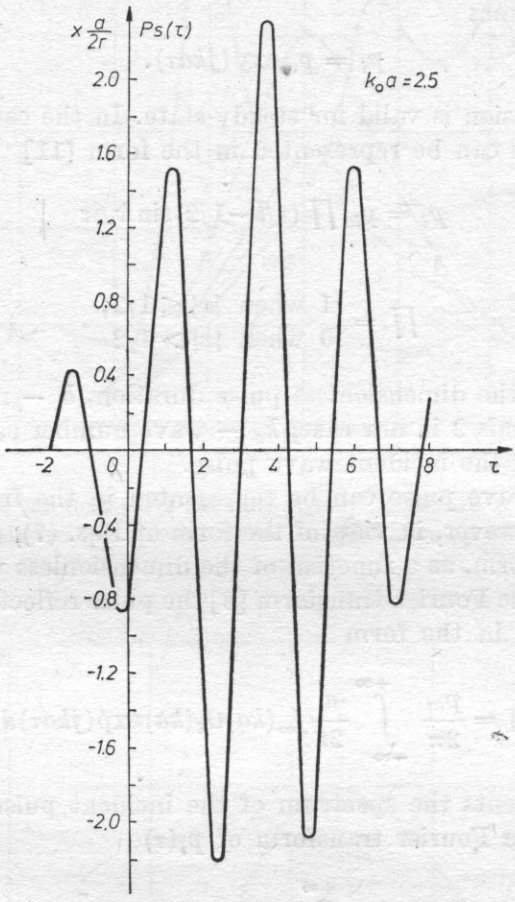

Fig. 3. Ultrasonic pulses reflected from elastic sphere under consideration for $k_0a = 2.5$

The frequency bandwidth of the incident wave pulse (between first zeros) falls within the interval (0.5–1.5) $\omega_0 = (0.5–1.5)\ k_0a$, where ω_0 denotes the angular carrier frequency of the pulse. It follows hence, that in the formation of integral (9) averaging of the function $f_\infty(ka)$ will occur over a large range of ka (see Fig. 1). In the case elastic sphere the function $f_\infty(ka)$ shows many peaks which correspond to many resonances occurring in the sphere. FLAX et al. [3] have shown that the scattering by elastic sphere is the superposition of the scattering by a rigid sphere and a number of resonances arising in the sphere. These resonances differ in character, since they correspond to different wave types, including also transverse waves, surface waves, of the "whispering gallery" type and so on.

Therefore, in the case of calcifications with irregular shapes and corrugated surfaces, one should expect that a number of resonances will not occur at all an average value of the function $f_\infty(ka)$ could, approximately, be taken as 1 for higher values of k_0a. This approximation signifies in practice that the calcification model of the rigid sphere is accepted in this case.

4. Determination of the tissue interference background level

Many echoes obtained at the boundary of fat, fibre and gland tissues and on their inhomogeneities form a tissue interference background which may mask echoes from small calcifications. To determine the tissue interference background level, measurements were performed in 100 femal normal breasts of 50 women 21–54 years old at a depth of $r = 4$ cm by means of an echoscope with a non-focused ultrasonic beam of 5 MHz frequency (transducer radius $a_t = 2.5$ mm). The level of the tissue interference background was found $D = 27$ dB higher than the electronic noise level of the echoscope. The standard deviation of a single measurement was equal to $\sigma = 8$ dB. The electronic noise level was equal to 10 μV corresponding to the level $N = -148$ dB in respect to the transmitter signal of 240 V (in pulse), assumed as the reference level of 0 dB. Thus the overall electrical dynamics of the echoscope equated $W = 148$ dB.

The measurement idea is illustrated in Fig. 4. Taking into account transducing losses $T = -15$ dB, attenuation losses $A = \alpha \cdot 2r$ [cm]$\cdot f$[MHz] $= 44$ dB diffraction losses of the beam equal to 4 dB (not shown in Fig. 4) and the measured level D, one obtains the remaining value of the overall electrical dynamics equal to $\Delta W = 58$ dB. This value is crucial for the detection ability of calcifications.

To show that the obtained experimental results is probable from the theoretical point of view, we introduced a hypothetic reflector formed by the surface of the half-space H (Fig. 4) with characteristic acoustic impedance $\varrho'c' = \varrho c + \Delta\varrho c$. It can be assumed that tissue interference echoes result from the reflections of the ultrasonic beam when it is incident perpediculary at the plane surface of the reflector H. Different breast tissues may have irregular boundaries, however, highest echoes will be received from these surface elements of tissue boundaries, which are plane perpendicular to the ultrasonic beam axis.

If we assume that the plane reflecting surface element of the tissue boundary has a form of a disc with the diameter d, then the echo signal S_E can be expressed by the formula

$$S_E = \left(\frac{d}{D_b}\right) \delta_q S_T \quad \text{for } d \leqslant D_b \tag{11}$$

where D_b denotes the ultrasonic beam diameter, S_T — transmitting signal, q — reflection coefficient equal to

$$q = (\varrho'c' - \varrho c)/(\varrho'c' + \varrho c) \cong \Delta\varrho c/2\varrho c. \tag{12}$$

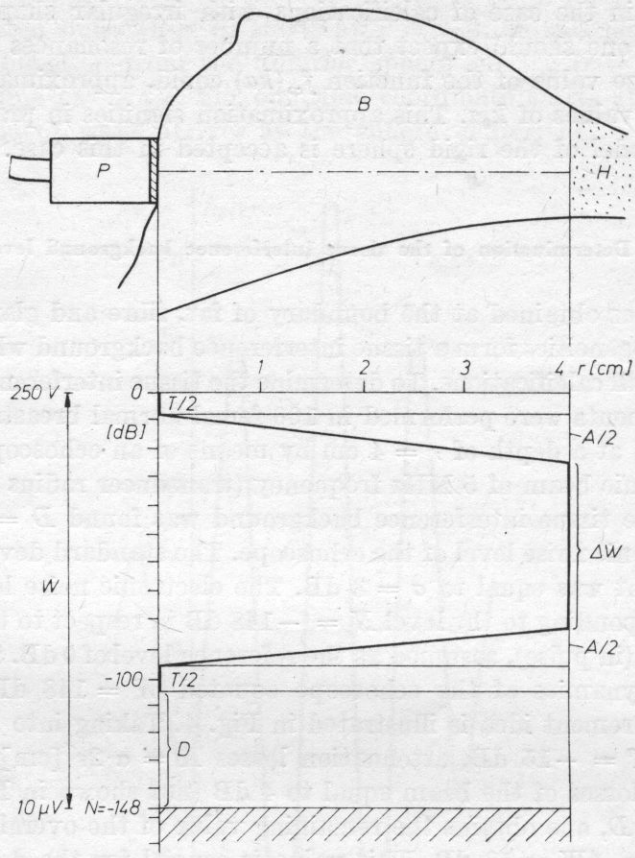

Fig. 4. The idea of the experimental determination of the tissue interference background level in womans breast: P — ultrasonic probe, B — breast, H — hypothetic reflector, O — level of the transmitting signal, T — transducing losses, A — attenuation losses in breast tissues, N — electronic noise level, W — electrical dynamics of the ultrasonograph, D — difference between the levels of the tissue interference background and the electronic noise, r — distance from the probe (depth)

The coefficient $\delta = \delta(r/l_0, d/D_b)$, depending on undulations in the ultrasonic field, can be found from the diagram determined experimentally by KRAUTKRÄMER [9], [10]. Its value tends to 1 for $r/l_0 \to 0$, where r is the distance between the reflector and the transducer, $l_0 = a_i^2/\lambda$ is the near field length. Eq. (11) is a generalized formula which for $q = 1$ was given and experimentally verified by KRAUTKRÄMER [9], [10]. For instance, in the case under consideration $D_b = 5$ mm, $d = 1$ mm, $r = 40$ mm, $l_0 = 21$ mm. For $r/l_0 = 2$ and $d/D_b = 0.2$ the coefficient $\delta = 1.8 - 5$ dB [10]. If one assumes for breast tissues $\Delta\varrho c/\varrho c = 5\,\%$ then Eqs. (13) and (14) give

$$S_E/S_T = 0.0018 = -55 \text{ dB}. \tag{13}$$

In this way we have shown that a small plane surface element of the tissue boundary, with the diameter of $d = 1$ mm, gives in uor case a maximum echo signal which is 55 dB lower than the transmitting signal S_T, incident at our hypothetic reflector. It means, that the resulting value $-\Delta W = S_E/S_T = -58$ dB obtained in measurements of the tissue interference background, seems to be most probable.

Now, equating ΔW to the ratio P_{s0}/P_{i0} one obtains from Eq. (4) the relation

$$\Delta W = \frac{a_m}{2r} f_\infty(ka_m) \tag{14}$$

where a_m denotes the radius of the calcification which given an echo on the level of the tissue interference background.

Table 2

r [cm]	R		$E(v = 0.2)$		R		R	
	a_m [mm]	ka	a_m [mm]	ka	$a_{2\sigma}$ [mm]	ka	$a_{3\sigma}$ [mm]	ka
2	0.09	1.9	0.085	1.77	0.4	8.5	1.0	21
4	0.1	2.25	0.09	1.9	0.6	13	1.6	34
6	0.11	2.25	0.09	1.93	0.7	14	1.7	35

If we assume that this level depends on the distance r according to the diagram of KRAUTKRÄMER [9] then ΔW for $r = 2$ cm is 4 dB greater and for $r = 6$ cm is 5 dB smaller than that one determined experimentally for the distance $r = 4$ cm. In this way one can find a_m from Eq. (14) for various values of r. Results of the calculations are shown in Table 2 for rigid and elastic spherical models of calcifications. The far field form function $f_\infty(ka)$ presented in Figs. 1 and 2 was applied in these computations.

It seems reasonable to assume the maximum error of single measurement of the tissue interference background to be 2σ or even 3σ. Then, according to the theory of error estimation [8] in the first case 97.72 % of all the values of $D = 27$ dB are smaller than $D+2\sigma = 43$ dB; the last value corresponding to $\Delta W = -42$ dB; in calcification detection to be certain, we assumed these limiting values in our calculations, thus determining the overestimated radius $a_{2\sigma}$ of the calcification which gives echoes higher by $2\sigma = 16$ dB (6.5 times) than the mean level of the tissue interference background. This seems to be necessary as in the case of small calcifications only the echo amplitude and no additional information e.g., on the shape, can be obtained. For the maximum error of 3σ one obtains the above values equal to 99.86 % and $\Delta W = -34$ dB, respectively.

Fig. 5 shows ultrasonic pulses reflected from elastic spherical calcifications, computed from Eqs. (9), (10), (5) and (8) for $k_0a = 5$ and 10. Their relative amplitudes are equal to 0.7 and 0.8, while those ones for the reflected continuous wave would be 1 (for $f_\infty(ka) = 1$). Thus the far field form function $f_\infty(ka)$ can be for $ka = 5$ or 10 approximated by the value of 1 giving an error in amplitude of 2 and 3 dB, respectively which can be neglected in our estimations. However, it is interesting to notice a great distortion of the shape of these reflected pulses.

5. Conclusions

Microcalcifications in the breast can not be detected with the ultrasonic echo method. The detectability is restricted by the tissue heterogeneities which constitute the background of tissue interference signals. The level of these signals was determined experimentally in 100 femal breasts. Assuming rigid and elastic spherical models, the radius of calcification which gives the same signal level was estimated to be $a_m = 0.1$ at the distance $r = 4$ cm and at the frequency of 5 MHz (standard deviation $\sigma = 8$ dB). This value does not depend distinctly on the distance $r = 2$–6 cm. For maximum sampling error 2σ and 3σ, assumed for a single measurement of the tissue interference background, the radii of detectable calcifications are equal to $a_{2\sigma} = 0.6$ mm and $a_{3\sigma} = 1.6$ mm, respectively.

a)

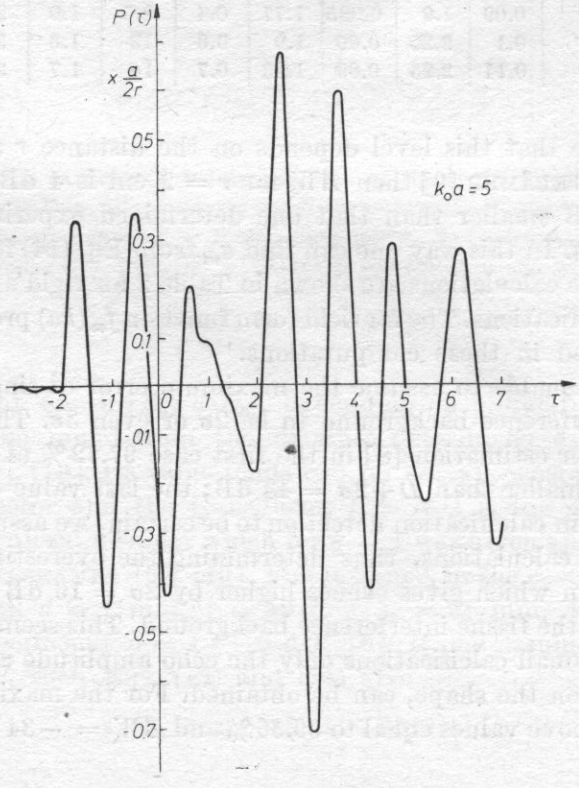

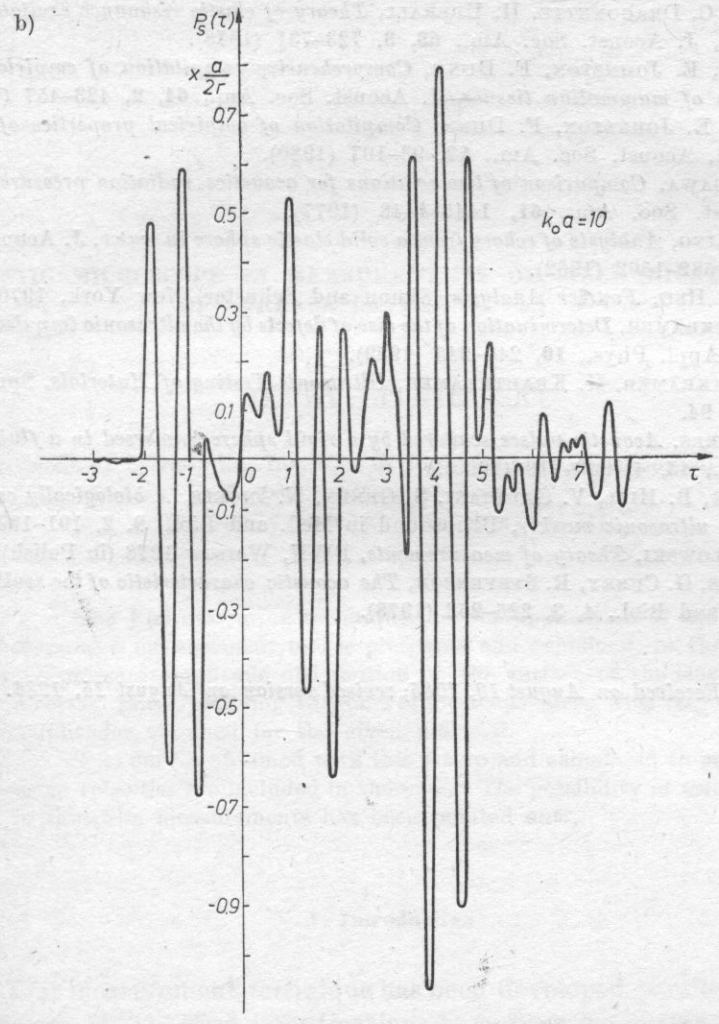

Fig. 5. Ultrasonic pulses reflected from elastic spheres under considerations for $k_0a = 5$ (a) and $k_0a = 10$ (b)

Both, rigid and elastic models give similar estimation results of calcification size. Therefore, it seems to be useful to apply the rigid spherical calcification model, in further research, as it is much simpler for computation than the elastic one.

References

[1] L. Filipczyński, *Detectability of calcifications in breast tissues by the ultrasonic echo method*, Archives of Acoustics, **8**, 3, 203–220 (1983).

[2] L. Filipczyński, G. Łypacewicz, *Estimation of calcification detectability in breast tissues by means of the ultrasonic echo and shadow method*, Archives of Acoustics, **9**, 1–2, 41–50 (1984).

[3] L. FLAX, C. DRAGONETTE, H. UBERALL, *Theory of elastic resonance excitation by sound scattering*, J. Acoust. Soc. Am., **63**, 3, 723–731 (1978).

[4] S. GROSS, E. JOHNSTON, F. DUNN, *Comprehensive compilation of empirical ultrasonic properties of mammalian tissues*, J. Acoust. Soc. Am., **64**, 2, 423–457 (1978).

[5] J. GOSS, E. JOHNSTON, F. DUNN, *Compilation of empirical properties of mammalian tissues*, J. Acoust. Soc. Am., **68**, 93–107 (1980).

[6] T. HASEGAWA, *Comparison of two solutions for acoustics radiation pressure on a sphere*, J. Acoust. Soc. Am., **61**, 1445–1448 (1977).

[7] R. HICKLING, *Analysis of echoes from a solid elastic sphere in water*, J. Acoust. Soc. Am., **34**, 10, 1582–1592 (1962).

[8] P. HWEI HSU, *Fourier Analysis*, Simon and Schuster, New York, 1970, p. 74.

[9] J. KRAUTKRÄMER, *Determination of the size of defects by the ultrasonic impulse echo method*, Brit. J. Appl. Phys., **10**, 240–245 (1959).

[10] J. KRAUTKRÄMER, H. KRAUTKRÄMER, *Ultrasonic Testing of Materials*, Springer, Berlin 1983, p. 94.

[11] A. RUDGERS, *Acoustic pulses scattered by a rigid sphere immersed in a fluid*, J. Acoust. Soc. Am., **45**, 4, 900–919 (1969).

[12] R. STERN, B. HILL, V. GAUDIANI, S. GREEN, N. INGELS, *A biologically compatible implantable ultrasonic marker*, Ultrasound in Med. and Biol., **9**, 2, 191–199 (1983).

[13] H. SZYDŁOWSKI, *Theory of measurements*, PWN, Warsaw 1978 (in Polish).

[14] D. WHITE, G. CURRY, R. STEVENSON, *The acoustic characteristic of the scull*, Ultrasound in Med. and Biol., **4**, 3, 225–252 (1978).

Received on August 19, 1985; revised version on August 15, 1986.